

Phases Calibration of RIS Using Backpropagation Algorithm

Wei Zhang¹, Bin Zhou¹, Tianyi Zhang², Yi Jiang³, Zhiyong Bu¹

¹Shanghai Institute of Microsystem and Information Technology, Chinese Academy of Sciences, Shanghai, China

Email: {wzhang, bin.zhou, zhiyong.bu}@mail.sim.ac.cn

²Shanghai Radio Equipment Research Institute, Shanghai, China

Email: hm_zty@outlook.com

³School of Information Science and Technology, Fudan University, Shanghai, China

Email: yijiang@fudan.edu.cn

Abstract—Reconfigurable intelligent surface (RIS) technology has emerged in recent years as a promising solution to the ever-increasing demand for wireless communication capacity. In practice, however, elements of RIS may suffer from phase deviations, which need to be properly estimated and calibrated. This paper models the problem of over-the-air (OTA) estimation of the RIS elements as a quasi-neural network (QNN) so that the phase estimates can be obtained using the classic backpropagation (BP) algorithm. We also derive the Cramér Rao Bounds (CRBs) for the phases of the RIS elements as a benchmark of the proposed approach. The simulation results verify the effectiveness of the proposed algorithm by showing that the root mean square errors (RMSEs) of the phase estimates are close to the CRBs.

Index Terms—reconfigurable intelligent surface, quasi-neural network (QNN), backpropagation (BP), Cramér Rao Bound (CRB).

I. INTRODUCTION

In recent years, the reconfigurable intelligent surface (RIS) technology has been intensively researched for wireless communication, as it can adjust the phase coefficients of its elements to enhance the wireless link quality [1] [2] and to mitigate interferences [3]. While most of the existing works assume that the tunable phases of the RIS elements are precisely known *a priori*, they are unavoidably subject to deviations owing to manufacturing imperfection and aging, which has been shown in [4, Fig. 1]. In the previous work [5], the sum rate performance of the proposed RIS-assisted in-band full-duplex (RAIBFD) system is sensitive to the phase deviations of the RIS elements [5, Fig. 9]. Hence, estimating the phases before applying the RIS to a practical RAIBFD system is a prerequisite.

As related works, conventional array calibration has been widely investigated for phased array radar systems. The paper [6] proposed a so-called rotating element electric field vector (REV) method, which measures the power of received signal as one of phase shifters changes its phase between 0° and 180° to calibrate an individual antenna element of the phased array. As an improvement to the REV method, the paper [7]

considered the effect of phase shifter's phase deviations for more accurate calibration. To be more time-efficient, the paper [8] improved the single-element REV method by switching the phases of several elements simultaneously to measure the array power variations. The measured power variations are expanded into a Fourier series, whose coefficients can be used to obtain the amplitudes and phases of multiple antenna elements.

Calibration of phase shifter is also considered in multi-input multi-output (MIMO) systems. The paper [9] investigated the over-the-air (OTA) calibration of a phase shifter network (PSN) for mmWave massive MIMO communications, which assumed that phase deviations of phase shifter are the same across different gears. As an extension to [9], the paper [4] proposed an OTA PSN calibration method for hybrid MIMO systems given that phase deviations vary at different gears of a phase shifter. For the RIS elements of finite bit resolution, the phase deviations also need to be estimated and calibrated on different gears. The paper [10] proposed an OTA calibration algorithm of an M_{ris} -element RIS by iteratively estimating the channel and the phases of RIS, but it needs to calculate the inversion of an $M_{ris} \times M_{ris}$ matrix [10, (17)] and performs the iterative Riemannian conjugate gradient (RCG) algorithm in each iteration, yielding excessive computational complexity as M_{ris} grows larger.

In this paper, we propose to model the OTA phase estimation of the RIS elements into a QNN training problem, where the unknown phases and channel state information (CSI) become the weights of the proposed QNN. Then we utilize the backpropagation (BP) algorithm to train the QNN until the cost function converges and obtain the estimated phases. The simulation results verify the effectiveness of the proposed algorithm by showing that the root mean square errors (RMSEs) of the phase estimates closely approach the Cramér Rao Bounds (CRBs).

II. SIGNAL MODEL AND PROBLEM FORMULATION

A. Signal Model

Consider a single-input multi-output (SIMO) communication system comprised of a single-antenna transmitter, a receiver with M_r antennas, and a RIS with M_{ris} elements

Work in this paper was supported by Shanghai Post-doctoral Excellence Program Grant No. 2023689. The MATLAB codes are available: <https://github.com/henryforzhang/qnn-ris-calibration>.

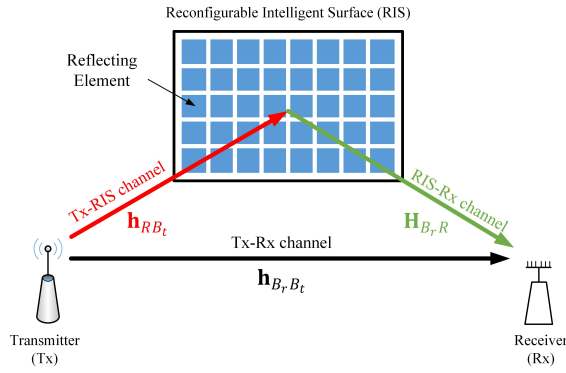


Fig. 1. Signal transmission model for RIS calibration.

as shown in Fig. 1, where $\mathbf{h}_{B_r B_t} \in \mathbb{C}^{M_r \times 1}$ is the channel from the transmitter to the receiver, $\mathbf{h}_{R B_t} \in \mathbb{C}^{M_{ris} \times 1}$ denotes the channel from the transmitter to the RIS, and $\mathbf{H}_{B_r R} \in \mathbb{C}^{M_r \times M_{ris}}$ represents the channel from RIS to the receiver. Given that the transmitter sends pilot sequence $\mathbf{s} \in \mathbb{C}^{N \times 1}$ and the RIS is turned on, the receiver receives

$$\mathbf{Y} = (\mathbf{H}_{B_r R} \mathbf{D} \mathbf{h}_{R B_t} + \mathbf{h}_{B_r B_t}) \mathbf{s}^H + \mathbf{Z}_{\text{on}}, \quad (1)$$

where $\mathbf{D} = \text{diag}(e^{j\phi_1}, e^{j\phi_2}, \dots, e^{j\phi_{M_{ris}}}) \in \mathbb{C}^{M_{ris} \times M_{ris}}$ and $\{\phi_m\}_{m=1}^{M_{ris}} \in [0, 2\pi]$; $|\mathbf{s}(n)| = 1, n = 1, 2, \dots, N$ and $\mathbb{E}\{\mathbf{s}\mathbf{s}^H\} = \mathbf{I}$. We can also turn off the RIS to remove the reflection path of RIS, and then the signal at the receiver becomes

$$\mathbf{Y} = \mathbf{h}_{B_r B_t} \mathbf{s}^H + \mathbf{Z}_{\text{off}}, \quad (2)$$

where $\mathbf{Z}_{\text{on}}, \mathbf{Z}_{\text{off}} \in \mathbb{C}^{M_r \times N}$ are complex Gaussian noise whose entries follows $\mathcal{CN}(0, \sigma^2)$; thus, the signal-to-noise-ratio is defined as $\text{SNR} \triangleq \frac{1}{\sigma^2}$.

B. Phase Deviations

For b -bit RIS, the nominal phase set of its elements is $\{\phi | \phi = (l-1)\Delta, l = 1, 2, \dots, L\}$ where $L = 2^b$ and $\Delta = \frac{2\pi}{L}$. In practice, however, the elements of the b -bit RIS have different phase deviations across the L gears due to manufactural imperfection and aging, and the phase shift of the m -th element at the l -th gear is [10]

$$\phi_{m,l} = (l-1)\Delta + \epsilon_{m,l}, \quad (3)$$

where $\epsilon_{m,l}$ denotes the phase deviations of the m -th element at the l -th gear. Thus the phase set of the M_{ris} elements can be denoted as a matrix $\mathcal{P} \in \mathbb{C}^{M_{ris} \times L}$, of which the (m, l) -th element is $\phi_{m,l}$. This paper aims to estimate \mathcal{P} to calibrate the RIS for further applications.

C. Problem Formulation

According to (1), the effective channel is estimated as

$$\hat{\mathbf{h}}_{\text{on}} = \frac{1}{N} \mathbf{Y} \mathbf{s} = \mathbf{H}_{B_r R} \mathbf{D} \mathbf{h}_{R B_t} + \mathbf{h}_{B_r B_t} + \frac{1}{N} \mathbf{Z}_{\text{on}} \mathbf{s}, \quad (4)$$

as the RIS is on. When the RIS is turned off, we have from (2) that

$$\hat{\mathbf{h}}_{\text{off}} = \mathbf{h}_{B_r B_t} + \frac{1}{N} \mathbf{Z}_{\text{off}} \mathbf{s}. \quad (5)$$

We can first estimate \mathbf{h}_{on} for Q times by changing the gears of the phase shifts on the RIS for Q times and obtain Q pairs of \mathbf{D}_q and $\hat{\mathbf{h}}_{\text{on},q}, q = 1, 2, \dots, Q$, and then estimate \mathbf{h}_{off} for Q times to obtain $\hat{\mathbf{h}}_{\text{off},q}, q = 1, 2, \dots, Q$, finally we obtain

$$\hat{\mathbf{h}}_q = \hat{\mathbf{h}}_{\text{on},q} - \hat{\mathbf{h}}_{\text{off},q} = \mathbf{H}_{B_r R} \mathbf{D}_q \mathbf{h}_{R B_t} + \mathbf{z}_q, q = 1, 2, \dots, Q, \quad (6)$$

where $\mathbf{z}_q \sim \mathcal{CN}(\mathbf{0}, \frac{2\sigma^2}{N} \mathbf{I})$ and the phases of $\mathbf{D}_q, q = 1, 2, \dots, Q$ are some entries of the phase set \mathcal{P} . We need to estimate \mathcal{P} by solving the non-convex problem

$$\min_{\mathcal{P}, \mathbf{H}_{B_r R}, \mathbf{h}_{R B_t}} \sum_{q=1}^Q \|\hat{\mathbf{h}}_q - \mathbf{H}_{B_r R} \mathbf{D}_q \mathbf{h}_{R B_t}\|_2^2. \quad (7)$$

III. ALGORITHM FOR ESTIMATING THE PHASES WITH DEVIATIONS

In this section, we first propose a simple way to select a suitable set of gears of the RIS elements in Q measurements; second, we model the RIS calibration problem into a quasi-neural network (QNN) training problem and adopt the well-known backpropagation (BP) algorithm to obtain the estimate of \mathcal{P} .

A. Gear Selection

Denoting $\mathbf{H}_{\text{cas}} = \mathbf{H}_{B_r R} \text{diag}(\mathbf{h}_{R B_t}) \in \mathbb{C}^{M_r \times M_{ris}}$, we have from (6) that

$$\hat{\mathbf{h}}_q = \mathbf{H}_{\text{cas}} \exp(j\phi_q) + \mathbf{z}_q, q = 1, 2, \dots, Q, \quad (8)$$

where $\phi_q(m) = \mathcal{P}(m, \mathbf{g}_q(m))$ and $\mathbf{g}_q \in \mathbb{C}^{M_{ris} \times 1}$ represents the gears of m elements of RIS in the q -th measurement. According to (8), we can reformulate (7) into

$$\min_{\mathcal{P}, \mathbf{H}} \sum_{q=1}^Q \|\hat{\mathbf{h}}_q - \mathbf{H}_{\text{cas}} \exp(j\phi_q)\|_2^2. \quad (9)$$

Then we need to decide $\mathbf{g}_q, q = 1, 2, \dots, Q$ for the Q measurements. Here we divide the Q measurements into O groups, each consisting of L measurements, i.e., $Q = OL$. In the o -th group of measurement, the L selected gears of m -th element are

$$\check{\mathbf{g}}_{o,m} = [\mathbf{g}_{(o-1)L+1}(m), \mathbf{g}_{(o-1)L+2}(m), \dots, \mathbf{g}_{(o-1)L+L}(m)]^T, \quad (10)$$

Letting each gear of the phase shifter appears just once in $\check{\mathbf{g}}_{o,m}$, we have

$$\check{\mathbf{g}}_{o,m} = \mathbf{\Pi}_{o,m} \mathbf{c} \in \mathbb{C}^{L \times 1}, \quad (11)$$

where $\mathbf{\Pi}_{o,m} \in \mathbb{C}^{L \times L}$ is a permutation matrix and $\mathbf{c} = [1, 2, \dots, L]^T \in \mathbb{C}^{L \times 1}$. According to (11), we can also obtain the L phases of m -th element as

$$\check{\phi}_{o,m} = \mathbf{\Pi}_{o,m} \psi_m \in \mathbb{C}^{L \times 1}, \quad (12)$$

where $\psi_m = [\phi_{m,1}, \phi_{m,2}, \dots, \phi_{m,L}]^T$ [cf. (3)]. The phases of the M_{ris} RIS elements in the o -th group can be denoted as

$$\check{\Phi}_o = [\check{\phi}_{o,1}, \check{\phi}_{o,2}, \dots, \check{\phi}_{o,M_{ris}}]^T \in \mathbb{C}^{M_{ris} \times L}. \quad (13)$$

Hence we can estimate LM_{ris} phases of the RIS with each phase being measured O times.

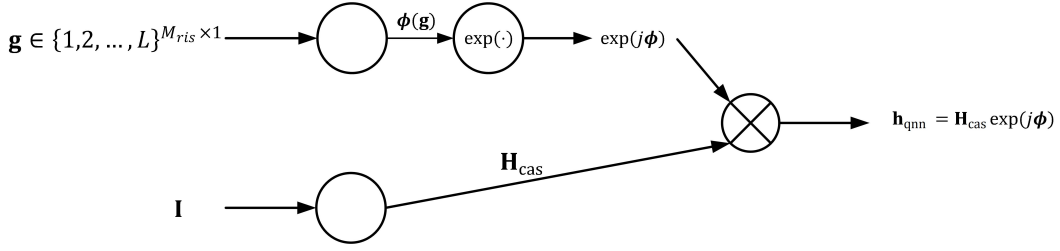


Fig. 2. The proposed quasi-neural network.

B. Quasi-Neural Network Formulation

We model the RIS calibration problem using a QNN as shown in Fig. 2, which has two inputs: one is the gear vector $\mathbf{g} \in \{1, 2, \dots, L\}^{M_{ris} \times 1}$; the other is a unit matrix \mathbf{I} . The upper branch yields the term $\exp(j\phi)$ and the lower branch yields \mathbf{H}_{cas} in Fig. 2, where $\exp(\cdot)$ acts as an activate function. Feeding \mathbf{g} and \mathbf{I} into the QNN, we have the output of the QNN as

$$\mathbf{h}_{qnn} = \mathbf{H}_{cas} \exp(j\phi). \quad (14)$$

The cost function of the proposed QNN is

$$C = \|\hat{\mathbf{h}}_q - \mathbf{h}_{qnn}\|_2^2, q = 1, 2, \dots, Q, \quad (15)$$

where the estimated effective channels $\hat{\mathbf{h}}_q, q = 1, 2, \dots, Q$ can be used as labels to train the QNN. Using the backpropagation (BP) algorithm, we can obtain the estimated \mathcal{P} as the cost function (15) converges.

C. Backpropagation Algorithm

The BP algorithm is based on the chain rules, which facilitate the calculation of gradients. To train the proposed QNN, we need to calculate the gradients $\frac{\partial C}{\partial \phi}$ and $\frac{\partial C}{\partial \mathbf{H}_{cas}^*}$, which is detailed as follows.

First, we calculate $\frac{\partial C}{\partial \phi}$. We have

$$\begin{aligned} \frac{\partial C}{\partial \phi} &= \frac{\partial C}{\partial \mathbf{h}_{qnn}} \frac{\partial \mathbf{h}_{qnn}}{\partial \phi} + \frac{\partial C}{\partial \mathbf{h}_{qnn}^*} \frac{\partial \mathbf{h}_{qnn}^*}{\partial \phi}, \\ &= 2\text{Re} \left[\frac{\partial C}{\partial \mathbf{h}_{qnn}} \frac{\partial \mathbf{h}_{qnn}}{\partial \phi} \right], \\ &= -2\text{Im} \left[(\mathbf{H}_{cas}^H (\hat{\mathbf{h}}_q - \mathbf{h}_{qnn})) \circ \exp(-j\phi) \right], \end{aligned} \quad (16)$$

where \circ represents the Hadamard product. Second, we have

$$\frac{\partial C}{\partial \mathbf{H}_{cas}^*} = (\mathbf{h}_{qnn} - \hat{\mathbf{h}}_q) \exp(-j\phi^T). \quad (17)$$

Then we can update \mathbf{H}_{cas} and ϕ as

$$\begin{aligned} \mathbf{H}_{cas}(t) &= \mathbf{H}_{cas}(t-1) - \lambda \frac{\partial C}{\partial \mathbf{H}_{cas}^*}(t), \\ \phi(t) &= \phi(t-1) - \lambda \frac{\partial C}{\partial \phi}(t), \end{aligned} \quad (18)$$

where λ is the learning rate and t is the iteration index for BP algorithm. Iterating t from 1 to ∞ until (15) improves less than ϵ , e.g., $\epsilon = 10^{-5}$, we can obtain the estimated phases $\hat{\mathcal{P}}$.

D. Complexity Analysis

We conclude the above procedure in Algorithm 1, and the computational complexity mainly lies in (16) and (17) in line 7, where (16) requires $M_r M_{ris} + \frac{1}{2} M_{ris}$ complex multiplications and (17) requires $M_r M_{ris}$ complex multiplications. Hence the complexity of each iteration is $\mathcal{O}(M_r M_{ris})$.

Algorithm 1 Algorithm for estimating the phases of the RIS

Input: Q gear vectors $\mathbf{g}_q, q = 1, 2, \dots, Q$; the effective channel $\hat{\mathbf{h}}_q$;

Output: The estimated phase set $\hat{\mathcal{P}}$;

1: Initialize the quasi-NN with random $\mathbf{H}_{cas}(0)$ and the nominal phase set $\mathcal{P}(0)$;

2: $t = 1$;

3: **do**

4: loss = 0

5: **for** $q = 1 : Q$ **do**

6: Calculate $\mathbf{h}_{qnn}(t)$ by (14) based on \mathbf{g}_q ;

7: Calculate $\frac{\partial C}{\partial \phi}(t), \frac{\partial C}{\partial \mathbf{H}_{cas}^*}(t)$ using (16) and (17);

8: Update $\phi(t)$ and $\mathbf{H}(t)$ using (18);

9: loss = loss + $\|\hat{\mathbf{h}}_q - \mathbf{h}_{qnn}(t)\|_2^2$;

10: $t = t + 1$;

11: **end for**

12: $C_{ave} = \text{loss}/Q$;

13: **while** C_{ave} improves less than ϵ .

IV. CRAMÉR RAO BOUND

In this section, we first analyze the phase ambiguity and then derive the CRB for the RIS calibration as a performance benchmark of the proposed algorithm.

A. Phase Ambiguity

We have from (8) that

$$\hat{\mathbf{h}}_q = (\mathbf{H}_{cas} \mathbf{T})(\mathbf{T}^H \exp(j\phi_q)) + \mathbf{z}_q, q = 1, 2, \dots, Q, \quad (19)$$

where $\mathbf{T} = \text{diag}(e^{j\varphi_1}, e^{j\varphi_2}, \dots, e^{j\varphi_{M_{ris}}})$ and $\{\varphi_m\}_{m=1}^{M_{ris}}$ are random phases. To remove the ambiguity brought by \mathbf{T} , we let $\varphi_m = \phi_{m,1}, m = 1, 2, \dots, M_{ris}$, based on which we derive the CRBs in the next subsection. According to (19), the number of unknown variables is $(2M_r + L - 1)M_{ris}$, while the number of constraints is $2LOM_r$. Thus we have

$$2LOM_r > (2M_r + L - 1)M_{ris}, \quad (20)$$

from which the lower bound of Q is

$$Q = OL \geq \left[M_{ris} + \frac{1}{2}(L-1) \frac{M_{ris}}{M_r} \right]. \quad (21)$$

B. Cramér Rao Bound

As the O groups of the measurements are independent, let us first focus on the o -th group to derive the CRB of the estimations related to the RIS calibration, and the unknown parameters are the vector

$$\boldsymbol{\eta} = \left[\boldsymbol{\Omega}^T, \text{Re}[\mathbf{h}_{cas}]^T, \text{Im}[\mathbf{h}_{cas}]^T \right]^T \in \mathbb{C}^{M_{ris}(L-1)+2M_r M_{ris}}, \quad (22)$$

where $\mathbf{h}_{cas} = \text{vec}(\mathbf{H}_{cas})$ and

$$\boldsymbol{\Omega} = [\phi_{1,2}, \phi_{1,3}, \dots, \phi_{1,L}, \dots, \phi_{M_{ris},2}, \dots, \phi_{M_{ris},L}]^T. \quad (23)$$

Combining (8) and (13) yields that

$$\check{\mathbf{H}}_o^T = \exp(j\check{\boldsymbol{\Phi}}_o^T) \mathbf{H}_{cas}^T + \mathbf{Z}_o^T \quad (24)$$

where

$$\begin{aligned} \check{\mathbf{H}}_o &= [\hat{\mathbf{h}}_{(o-1)L+1}, \hat{\mathbf{h}}_{(o-1)L+2}, \dots, \hat{\mathbf{h}}_{(o-1)L+L}], \\ \check{\mathbf{Z}}_o &= [\mathbf{z}_{(o-1)L+1}, \mathbf{z}_{(o-1)L+2}, \dots, \mathbf{z}_{(o-1)L+L}]. \end{aligned} \quad (25)$$

Using formula $\text{vec}(\mathbf{ABC}) = (\mathbf{C}^T \otimes \mathbf{A})\text{vec}(\mathbf{B})$, we have from (24) that

$$\check{\mathbf{h}}_o = (\mathbf{H}_{cas} \otimes \mathbf{I}_L) \exp(j\text{vec}(\check{\boldsymbol{\Phi}}_o^T)) + \check{\mathbf{z}}_o \quad (26)$$

where $\check{\mathbf{h}}_o = \text{vec}(\check{\mathbf{H}}_o^T)$ and $\check{\mathbf{z}}_o = \text{vec}(\check{\mathbf{Z}}_o^T)$. According to (12) and (13), we can further obtain

$$\begin{aligned} \text{vec}(\check{\boldsymbol{\Phi}}_o^T) &= [\check{\phi}_{o,1}^T, \check{\phi}_{o,2}^T, \dots, \check{\phi}_{o,M_{ris}}^T]^T \in \mathbb{C}^{LM_{ris} \times 1} \\ &= \boldsymbol{\Pi}_o \boldsymbol{\psi}, \end{aligned} \quad (27)$$

where

$$\begin{aligned} \boldsymbol{\Pi}_o &= \text{diag}(\boldsymbol{\Pi}_{o,1}, \boldsymbol{\Pi}_{o,2}, \dots, \boldsymbol{\Pi}_{o,M_{ris}}), \\ \boldsymbol{\psi} &= [\boldsymbol{\psi}_1^T, \boldsymbol{\psi}_2^T, \dots, \boldsymbol{\psi}_{M_{ris}}^T]^T. \end{aligned} \quad (28)$$

Hence inserting (27) into (26) yields that

$$\check{\mathbf{h}}_o = (\mathbf{H}_{cas} \otimes \mathbf{I}_L) \boldsymbol{\Pi}_o \boldsymbol{\psi} + \check{\mathbf{z}}_o \quad (29)$$

where $\check{\mathbf{h}}_o$ is of $\check{\mathbf{h}}_o \sim \mathcal{CN}(\boldsymbol{\mu}_o, \sigma_z^2 \mathbf{I})$ and $\boldsymbol{\mu}_o = (\mathbf{H}_{cas} \otimes \mathbf{I}) \boldsymbol{\Pi}_o \boldsymbol{\psi}$. The Fisher Information Matrix (FIM) is

$$\mathbf{F} = \frac{N}{\sigma^2} \sum_{o=1}^O \text{Re} \left[\frac{\partial \boldsymbol{\mu}_o^H(\boldsymbol{\eta})}{\partial \boldsymbol{\eta}} \frac{\partial \boldsymbol{\mu}_o(\boldsymbol{\eta})}{\partial \boldsymbol{\eta}} \right]. \quad (30)$$

As

$$\frac{\partial \boldsymbol{\mu}_o(\boldsymbol{\eta})}{\partial \boldsymbol{\eta}} = \left[\frac{\partial \boldsymbol{\mu}_o(\boldsymbol{\eta})}{\partial \boldsymbol{\Omega}}, \frac{\partial \boldsymbol{\mu}_o(\boldsymbol{\eta})}{\partial \text{Re}(\mathbf{h})}, \frac{\partial \boldsymbol{\mu}_o(\boldsymbol{\eta})}{\partial \text{Im}(\mathbf{h})} \right], \quad (31)$$

we can compute $\frac{\partial \boldsymbol{\mu}_o(\boldsymbol{\eta})}{\partial \boldsymbol{\eta}}$ in three parts. First, we compute $\frac{\partial \boldsymbol{\mu}_o(\boldsymbol{\eta})}{\partial \boldsymbol{\Omega}}$. Denoting $\mathbf{J}_o = j(\mathbf{H}_{cas} \otimes \mathbf{I}) \boldsymbol{\Pi}_o \text{diag}(\boldsymbol{\psi})$, we have

$$\frac{\partial \boldsymbol{\mu}_o(\boldsymbol{\eta})}{\partial \boldsymbol{\Omega}} = \mathbf{J}_o(:, \mathcal{I}), \quad (32)$$

where $\mathcal{I} = \{i | i = (m-1)L + (2:L), m = 1, 2, \dots, M_{ris}\}$. Second, we have

$$\frac{\partial \boldsymbol{\mu}_o(\boldsymbol{\eta})}{\partial \text{Re}(\mathbf{h}_{cas})} = [\mathbf{r}_{1,1}, \mathbf{r}_{2,1}, \dots, \mathbf{r}_{M_r,1}, \dots, \mathbf{r}_{M_r, M_{ris}}], \quad (33)$$

where

$$\mathbf{r}_{i,j} = \left[\begin{array}{c} \mathbf{0}_{L \times 1} \\ \vdots \\ \mathbf{0}_{L \times 1} \\ \boldsymbol{\Pi}_{o,j} \boldsymbol{\psi}_j \\ \mathbf{0}_{L \times 1} \\ \vdots \\ \mathbf{0}_{L \times 1} \end{array} \right] \begin{array}{l} \left. \vphantom{\begin{array}{c} \mathbf{0}_{L \times 1} \\ \vdots \\ \mathbf{0}_{L \times 1} \end{array}} \right\} i-1 \\ \left. \vphantom{\begin{array}{c} \boldsymbol{\Pi}_{o,j} \boldsymbol{\psi}_j \\ \mathbf{0}_{L \times 1} \\ \vdots \\ \mathbf{0}_{L \times 1} \end{array}} \right\} M_r - i \end{array}, \quad (34)$$

for $i = 1, 2, \dots, M_r$ and $j = 1, 2, \dots, M_{ris}$. Third, we have

$$\frac{\partial \boldsymbol{\mu}_o(\boldsymbol{\eta})}{\partial \text{Im}(\mathbf{h}_{cas})} = j \frac{\partial \boldsymbol{\mu}_o(\boldsymbol{\eta})}{\partial \text{Re}(\mathbf{h}_{cas})}. \quad (35)$$

Then inserting (32), (33), and (35) into (31), we have $\frac{\partial \boldsymbol{\mu}_o(\boldsymbol{\eta})}{\partial \boldsymbol{\eta}}$, from which we can obtain the FIM from (30). Thus, the CRB is $\mathbf{C}\boldsymbol{\eta} = \mathbf{F}^{-1}$, of which the first $M_{ris}(L-1)$ diagonal elements is the CRBs of $\boldsymbol{\Omega}$.

V. NUMERICAL EXAMPLES

In this section, we provide some simulation results to verify the effectiveness of the proposed algorithm. The pilot length is 100, i.e., $N = 100$; the permutation matrices are randomly generated; we consider a 4-bit RIS whose phase deviations are uniformly distributed between $[-20^\circ, 20^\circ]$ [4, Fig. 1]; the learning rate λ is set to be 5×10^{-3} . The entries of $\mathbf{h}_{B_r B_t}$, $\mathbf{h}_{R B_t}$, and $\mathbf{H}_{B_r R}$ are obtained from the Saleh-Valenzuela model [11].

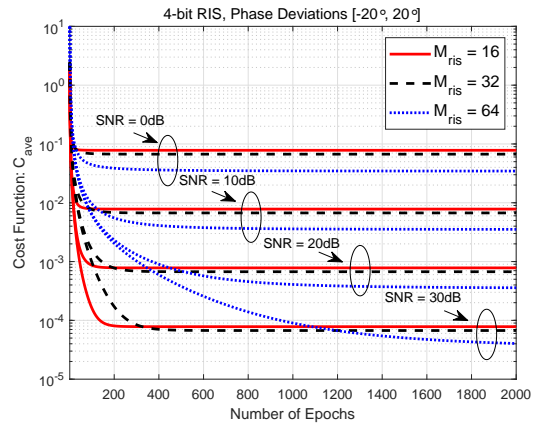


Fig. 3. The convergence performance of the proposed algorithm.

In the first example, we simulate the convergence performance of the proposed algorithm using RIS with size of 2×8 , 4×8 , and 8×8 in Fig. 3, where the QNN is trained with all Q samples of the training set once in one epoch. Each phase of the 4-bit RIS is measured $O = 15$ times, thus the training set contains $Q = 15 \times 2^4 = 240$ samples. The number

of antennas at the receiver is $M_r = 4$. Fig. 3 shows that the cost function value C_{ave} can achieve a smaller value as SNR varies from 0dB to 30dB, where C_{ave} is defined in line 12 of Algorithm 1. Similar to the conventional neural network, the algorithm with RIS of larger size, i.e., 8×8 RIS, tends to converge much slower than that with RIS size of 2×8 and 4×8 as more weights need to be trained.

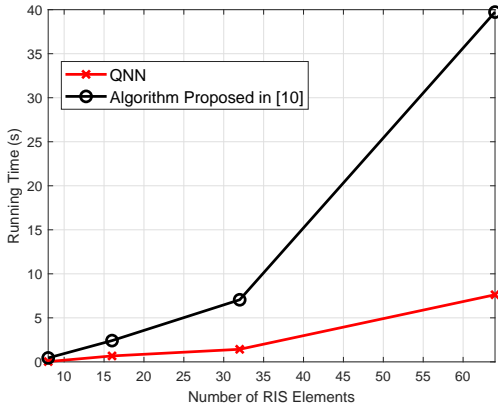


Fig. 4. RMSE and running time vs. M_{ris} with $O = 15$ and SNR = 20dB.

The second simulation studies the MATLAB (MATLAB R2020b) running time of the proposed BP algorithm, and compares it with that of the algorithm proposed in [10] given that where $M_r = 8$. The simulation is conducted on a Windows 10 computer equipped with AMD Ryzen 7 Pro 4750G. According to Fig. 4, the proposed algorithm takes much less MATLAB running time. That's because the number of optimized variables and the computational complexity in each iteration of the proposed BP algorithm is M_{ris} and $\mathcal{O}(M_r M_{ris})$ rather than LM_{ris} and $\mathcal{O}(M_{ris}^3)$ in [10].

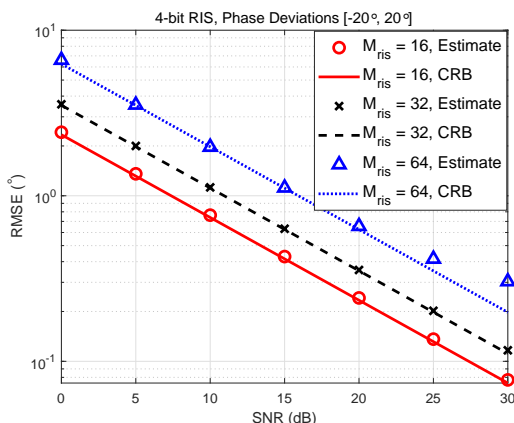


Fig. 5. RMSE and CRB vs. SNR with $O = 15$.

The third example studies the RMSE performance of the proposed algorithm as the SNR varies from 0dB to 30dB,

where the RMSE is defined as

$$\text{RMSE} \triangleq \sqrt{\frac{\mathbb{E}\{\|\hat{\Omega} - \Omega\|_2^2\}}{(L-1)M_{ris}}} \times \frac{180^\circ}{\pi}.$$

Fig. 5 shares the same simulation settings with Fig. 3 and shows the RMSEs of the estimated phases are close to the CRBs with $M_{ris} = 16, 32, 64$. But for RIS of larger size, e.g., 8×8 RIS, the proposed algorithm tends to converge at a locally optimal point at SNR = 30dB, and hence the RMSE slightly deviates from the CRB.

VI. CONCLUSION

This paper proposes to model the estimation of the RIS phase with deviations into a quasi-neural network (QNN) training problem and utilize the backpropagation (BP) algorithm to train the QNN, which can estimate the phases of the RIS elements at each gear given unknown channel state information (CSI). We also derive the Cramér Rao Bounds (CRBs) for the RIS calibration as a benchmark of the proposed approach. The simulation results verify the effectiveness of the proposed algorithm as the root mean square errors (RMSEs) of the phase estimates are close to the Cramér Rao Bounds (CRBs), and show its superior performance in computation complexity over the state-of-the-art technique.

REFERENCES

- [1] T. J. Cui, M. Q. Qi, X. Wan, J. Zhao, and Q. Cheng, "Coding metamaterials, digital metamaterials and programmable metamaterials," *Light Science & Applications*, vol. 3, no. 10, 2014.
- [2] Y. Liu, X. Liu, X. Mu, T. Hou, J. Xu, M. Di Renzo, and N. Al-Dhahir, "Reconfigurable intelligent surfaces: Principles and opportunities," *IEEE Communications Surveys & Tutorials*, vol. 23, no. 3, pp. 1546–1577, 2021.
- [3] S. Tewes, M. Heinrichs, P. Staat, R. Kronberger, and A. Sezgin, "Full-duplex meets reconfigurable surfaces: RIS-assisted SIC for full-duplex radios," in *ICC 2022 - IEEE International Conference on Communications*, 2022, pp. 1106–1111.
- [4] W. Zhang and Y. Jiang, "Over-the-air calibration of phase shifter network for hybrid MIMO systems," *IEEE Transactions on Signal Processing*, vol. 70, pp. 3456–3467, 2022.
- [5] W. Zhang, Z. Wen, C. Du, Y. Jiang, and B. Zhou, "RIS-assisted self-interference mitigation for in-band full-duplex transceivers," *IEEE Transactions on Communications*, vol. 71, no. 9, pp. 5444–5454, 2023.
- [6] S. Mano and T. Katagi, "A method for measuring amplitude and phase of each radiating element of a phased array antenna," *Electronics and Communications in Japan (Part I: Communications)*, vol. 65, no. 5, pp. 58–64, 1982.
- [7] N. Takemura, H. Deguchi, R. Yonezawa, and I. Chiba, "Phased array calibration method with evaluating phase shifter error," in *Proceedings of the international Symposium on Antennas and Propagation Japan*, vol. 3, 2000, pp. 1171–1174.
- [8] T. Takahashi, Y. Konishi, S. Makino, H. Ohmine, and H. Nakaguro, "Fast measurement technique for phased array calibration," *IEEE Transactions on Antennas and Propagation*, vol. 56, no. 7, pp. 1888–1899, 2008.
- [9] X. Wei, Y. Jiang, Q. Liu, and X. Wang, "Calibration of phase shifter network for hybrid beamforming in mmWave massive MIMO systems," *IEEE Transactions on Signal Processing*, vol. 68, pp. 2302–2315, 2020.
- [10] W. Zhang and Y. Jiang, "Over-the-air phase calibration of reconfigurable intelligent surfaces," *IEEE Wireless Communications Letters*, vol. 12, no. 4, pp. 664–668, 2023.
- [11] T. Rappaport, R. Heath, R. Daniels, and J. Murdock, *Millimeter wave wireless communications*. Prentice Hall, 2015.